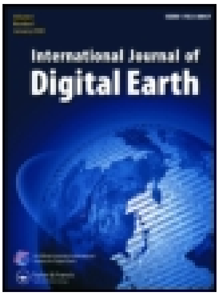

International Journal of Digital Earth
Publication details, including instructions for authors and subscription information:
http://www.tandfonline.com/loi/tjde20

Remote determination of chromophoric dissolved organic matter in lakes, China

Guangjia Jiang [a b] , Ronghua Ma [a] , Hongtao Duan [a] , Steven A. Loiselle [c] , Jingping Xu [d] & Dianwei Liu [d]

[a] State Key Laboratory of Lake Science and Environment , Nanjing Institute of Geography and Limnology, Chinese Academy of Sciences , Nanjing , China

[b] University of Chinese Academy of Sciences , Beijing , China

[c] Dipartimento Farmaco Chimico Tecnologico , CSGI, University of Siena , Siena , Italy

[d] Northeast Institute of Geography and Agricultural Ecology , Chinese Academy of Sciences , Changchun , China

Published online: 03 Jul 2013.

International Journal of Digital Earth, 2013
http://dx.doi.org/10.1080/17538947.2013.805261

Remote determination of chromophoric dissolved organic matter in lakes, China

Guangjia Jiang[a,b], Ronghua Ma[a]*, Hongtao Duan[a], Steven A. Loiselle[c], Jingping Xu[d] and Dianwei Liu[d]

[a]*State Key Laboratory of Lake Science and Environment, Nanjing Institute of Geography and Limnology, Chinese Academy of Sciences, Nanjing, China;* [b]*University of Chinese Academy of Sciences, Beijing, China;* [c]*Dipartimento Farmaco Chimico Tecnologico, CSGI, University of Siena, Siena, Italy;* [d]*Northeast Institute of Geography and Agricultural Ecology, Chinese Academy of Sciences, Changchun, China*

(*Received 15 August 2012; final version received 9 May 2013*)

Chromophoric dissolved organic matter (CDOM) strongly influences the water-leaving radiance from aquatic ecosystems. In most inland waters, the remote determination of CDOM absorption presents a central challenge due to their complex optical conditions. However, identifying the temporal and spatial variability of CDOM is fundamental to the understanding of aquatic biogeochemical dynamics. In the present study, semi-analytical and empirical modeling approaches were used to examine CDOM absorption in four, shallow, inland water bodies using the spectral bands and sensitivities of major satellite observational systems. Of the models examined, an empirical multiband model was found to provide the highest correlation with measured CDOM absorption. The spectral characteristics of the MERIS sensors yielded the best results with respect to the other available satellite sensors. High detrital load was observed to be a major impediment to estimating CDOM absorption, while lakes with elevated phytoplankton biomass did not present similar problems.

Keywords: inland waters; remote sensing; lake carbon; DOC; absorption

1. Introduction

The water-leaving radiance from natural waters is influenced by the characteristics of the optically active components of the water body and the distribution of the incident radiance. Chromophoric dissolved organic matter (CDOM), also known as Gelbstoff (Kirk 1976; Morel 1988), is the optically active fraction of the dissolved organic carbon pool. It is a complex mixture of aliphatic and aromatic polymers, which have an increasing absorption in the ultraviolet and short visible wavelengths (Stedmon, Markager, and Bro 2003; Loiselle et al. 2010). This has important implications for biological, chemical and optical processes in aquatic systems. CDOM absorption can overlap with the absorption spectra of several photosynthetic pigments (Miller et al. 2002), influencing primary production (Kowalczuk et al. 2003). On the other hand, CDOM absorption offers protection of phytoplankton and other aquatic biota from the harmful UV radiance exposure (Loiselle et al. 2010). Therefore, it is important to

*Corresponding author. Email: mrhua2002@niglas.ac.cn

quantify the temporal and spatial distribution of CDOM with respect to the biological and geochemical processes that influence its variability.

Water 'color' can be determined quantitatively from the spectral backscattering intensity from the optically effective depth of the water column (Ma et al. 2011). Variations of water color can be associated to changes in inherent optical properties (IOPs) such as, the total absorption coefficient a, and the total backscattering coefficient b_b, which are directly related to the quantity and quality of the optically active substances present as:

$$a(\lambda) \approx a_w(\lambda) + a_{CDOM}(\lambda) + a_d(\lambda) + a_{ph}(\lambda) \quad (1)$$

where the total absorption coefficient ($a(\lambda)$, m^{-1}) is generally the sum of the absorption due to water (a_w), CDOM (a_{CDOM}), detritus (a_d) and phytoplankton (a_{ph}). The total backscattering coefficient ($b_b(\lambda)$, m^{-1}) can be described as the sum of backscattering related to: pure water (b_{bw}), detrital material (b_{bd}) and phytoplankton (b_{bph}):

$$b_b(\lambda) = b_{bw}(\lambda) + b_{bd}(\lambda) + b_{bph}(\lambda) \quad (2)$$

It should be noted that the absorption spectra of organic particulate detritus and CDOM are similar, both decreasing monotonically with the increasing wavelength (Briucaud, Morel, and Prieur 1981). This makes it difficult to separate their effect on upwelling radiance. In some cases, they are combined under the denomination of colored detrital material (CDM) (Bélanger, Babin, and Larouche 2008). However, CDOM is critical for quantifying photochemically induced biogeochemical processes (Siegel et al. 2002). For example, CDOM absorption will decrease with increasing exposure to ultraviolet irradiance, with important consequences on the photoproduction of atmospherically important radiative gases CO_2 and CO (Loiselle et al. 2012).

In general, quantitative and qualitative assessment of CDOM absorption by remote sensing is based on either empirical or semi-analytical approaches using reflectance measurements in specific bands within the visible spectrum. Successful results on the remote estimation of CDOM have been mostly focused on marine ecosystems (Morel and Gentili 2009). Common remote sensing algorithms in ocean color employ band-ratios of reflectance at specific wavelengths in the visible domain (Yu et al. 2010). Recently, a new semi-analytical methodology based on the Quasi Analytical Algorithm (QAA) (Lee, Carder, and Arnone 2002), named QAA-CDOM (Zhu and Yu 2012), was developed to estimate CDOM distribution in turbid estuarine and coastal regions. However, the estimation of IOPs is most difficult in the complex optical conditions of Case 2 waters, where the overall optical properties of the water are influenced not only by phytoplankton biomass, but also by other suspended particles and CDOM (Morel and Prieur 1977), which usually have multiple processes that modify the biological and geochemical properties of DOM (dilution, photodegradation, flocculation) (Loiselle et al. 2010). Different CDOM sources and loss processes will present spatially and spectrally distinct CDOM absorption properties. For example, the autochthonous CDOM (derived from algae and macrophytes) will have different optical characteristics than allochthonous CDOM (derived from organic soil and humic substances) (Yu et al. 2010).

The main objective of the present study was to test several semi-analytical and empirical modeling approaches to estimate CDOM absorption in complex inland water bodies. These approaches were explored using reflectance from field data in the spectral bands and sensitivities of the major satellite observational systems presently available. The most appropriate model was then used to remotely estimate the distribution of CDOM absorption in Taihu Lake using satellite measured reflectance from a single MERIS scene.

2. Material and methods

2.1. Study areas

In situ experiments were performed in four inland water bodies: Poyang Lake, Taihu Lake, Chaohu Lake and Shitoukoumen Reservoir (Figure 1, Table 1). Poyang Lake is the largest freshwater lake in China (Ma et al. 2010) and characterized by significant seasonal water level fluctuations with low dissolved organic matter (Li et al. 2010). Taihu Lake has been strongly affected by human activities and is characterized by

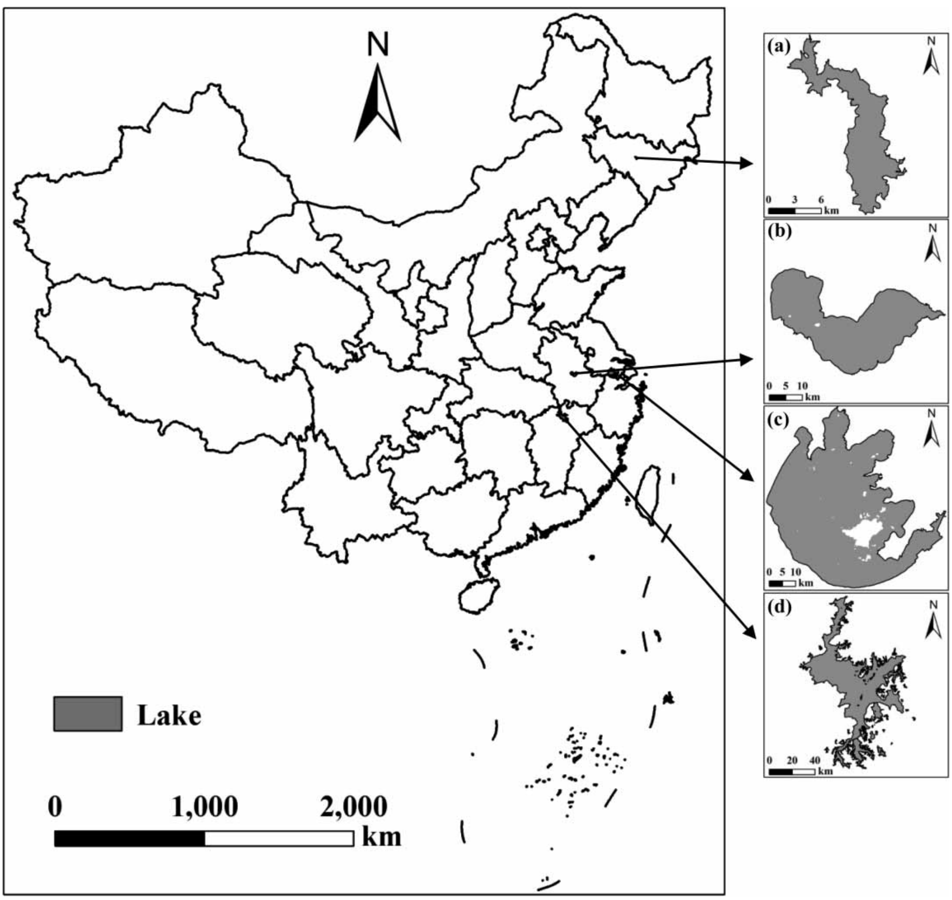

Figure 1. The four study lakes: (a) Shitoukoumen Reservoir; (b) Chaohu Lake; (c) Taihu Lake; (d) Poyang Lake.

Table 1. Sampling campaigns in the four study lakes.

Location	Area (km^2)	Depth (m)	Sampling Date	Proxy	Samples
Taihu Lake	2338	2.12	Oct. 18–Oct. 29, 2004	T(2004)	67
			Oct. 06–Oct. 17, 2008	T(2008)	145
			Apr. 23–May. 02, 2010	T(2010)	85
Chaohu Lake	769.5	2.69	Oct. 15–Oct. 16, 2009	C(2009)	37
Poyang Lake	3283	8.4	Oct. 15–Oct. 17, 2010	P(2010)	47
Shitoukoumen Reservior	94	3.3	Jun. 13, 2008	S(2008)	40
			Sep. 23, 2008		

eutrophic conditions and summertime cyanobacteria blooms (Duan et al. 2009), which resulted in heavy algae-derived CDOM being produced. Allochthonous CDOM inflows into the lake during the spring and summer flood season have been documented (Yao et al. 2011). Chaohu Lake in south China is a large hypereutrophic lake, characterized by extensive summertime cyanobacterial blooms with autochthonous CDOM sources and seasonal inflows of CDOM-rich waters from the surrounding rivers (Xie et al. 2005). Shitoukoumen Reservoir, a eutrophic reservoir in the northeast of China, has high concentrations of degradable dissolved organic matter (Jiang et al. 2010).

2.2. Field data

Geo-referenced field data (421 stations) were obtained during seven cruises in the four water bodies (Table 1). The biological and optical properties of the discrete water samples were measured in the laboratory analyses (Table 2). The above-surface remote sensing reflectance of water between 350 and 1050 nm (1 nm resolution) was measured with a FieldSpec Pro Dual VNIR (ASD, USA) following NASA protocols (Mueller, Fargion, and Mcclain 2003). The boat was positioned to avoid white caps and boat shadows.

Radiance from the water surface (L_t), denoting the total upwelling radiance into the detector, was measured using an ASD spectroradiometer which was mounted on the boat and equipped with a 4 m fiber optic cable. Measurements were made from 09:30 to 14:30 local time in sunny conditions with low wind speed ($<$ 3 m/s).

Upwelling radiance is dominated by the sum of the water-leaving radiance (L_w) and the reflected skylight into the direction of the sensor (L_r) (Mobley 1999):

$$L_t = L_w + L_r \tag{3}$$

where $L_r \approx \rho L_{s.}$ L_s is the sky diffuse radiance, which can be directly measured by the upward directed spectroradiometer and ρ represents the proportionality factor that relates L_s to the reflected sky radiance measured when the detector views the water surface. L_r is affected by wind speed, solar zenith angle and viewing geometry (Mobley 1999). The ρ term was calculated individually for every data by Hydro-Light, and ρ generally falls in the range of 0.026 to 0.028 for measurements made in the central part of the day. We used the average value, $\rho = 0.028$, for this study.

Table 2. Measured biological and optical properties of water samples during the six sampling campaigns in Shitoukoumen Reservoir (S), Chaohu Lake (C), Taihu Lake (T), and Poyang Lake (P).

	TSS (mg/l)			OSS (mg/l)			ISS (mg/l)			Chla (μg/l)			$a_{CDOM}(375)$ (m^{-1})		
	MIN	MAX	AVE	MIN	MAX	AVE	MIN	MAX	AVE	MIN	MAX	AVE	MIN	MAX	AVE
T(2004)	3.10	169.47	46.54	0.85	22.07	8.93	2.23	147.40	37.61	1.18	52.43	14.08	1.30	4.45	2.62
T(2008)	0.80	246.00	36.11	1.00	218.00	14.79	0.50	71.10	22.21	0.46	685.14	40.29	1.11	4.30	2.14
T(2010)	9.90	162.73	41.10	1.98	19.65	7.96	7.68	145.60	33.36	0.13	46.98	9.22	1.14	3.42	1.93
C(2009)	12.50	942.00	93.45	2.50	888.00	69.84	8.50	67.00	23.61	6.43	3580.27	377.45	0.74	21.61	4.73
P(2010)	19.00	168.00	57.96	3.60	20.00	8.03	13.00	148.00	49.93	1.47	24.65	8.39	0.83	2.14	1.44
S(2008)	12.50	121.00	31.91	ND	ND	ND	ND	ND	ND	12.90	47.52	30.00	1.84	13.24	4.65

ND, no data.

Remote sensing reflectance (R_{rs}) was determined by comparing the water-leaving radiance (L_w) to the downwelling irradiance ($E_d(0^+)$) just above water surface (Yu et al. 2010),

$$R_{rs} = L_w / E_d(0^+) \tag{4}$$

where $E_d(0^+)$ was estimated by measuring the upward directed radiance directly measuring the reflected radiance from the diffusely reflecting surface panel, L_g, from a diffusely reflecting surface as,

$$E_d(0^+) = L_g \pi / R_g \tag{5}$$

and R_g is the known reflectance of diffusely reflecting surface panel.

Inherent optical properties were measured from samples taken at a depth of 0.05m in each sampling site. Transmittance was measured with a UV2401 spectrophotometer after filtering water samples onto the 47-mm Whatman GF/F filters (pore size 0.7μm) at low vacuum. The absorbance of the filters rinsed with Milli-Q water was used as a reference. The total particulate absorption coefficient, $a_p(\lambda)$, was calculated using the Quantitative Filter pad Technique (QFT) following the NASA protocol (Mueller, Fargion, and Mcclain 2003). Non-pigment related spectral absorption ($a_d(\lambda)$) was determined by scanning the same filters after soaking for 60 minutes in sodium hypochlorite and using the Quantitative Filter pad Technique (QFT) (Mueller, Fargion, and Mcclain 2003). The difference between $a_p(\lambda)$ and $a_d(\lambda)$ provided the pigment absorption coefficient ($a_{ph}(\lambda)$). Final absorptions were corrected for internal backscattering by subtracting the absorption coefficients at 780 nm from all other wavelengths (Lee and Carder 2004).

Water samples were filtered under low vacuum through 0.22 μm Millipore filters pre-rinsed with Milli-Q water, and the filtrate was stored in amber-colored glass bottles at 4 °C for CDOM absorption measurement. CDOM absorbance was recorded from 250 to 800 nm (1 nm resolution) with a UV2401 spectrophotometer. The measured absorbance ($A(\lambda)$) was converted to absorption (a_{CDOM}, m^{-1}) according to $a_{CDOM}(\lambda) = 2.303A(\lambda)/l$, where l is the cuvette path length (1cm) (Del Castillo and Miller 2008). To describe the spatial and temporal variations in CDOM, the absorption coefficient at 375 nm ($a_{CDOM}(375)$ m^{-1}) was used.

Pigment samples were extracted in 90% ethanol, and chlorophyll-a concentration (Chla) was quantified using spectrophotometric measurements (Duan et al. 2010). The concentrations of total suspended solids (TSS), organic suspended solids (OSS), and inorganic suspended solids (ISS) were determined gravimetrically (Gersberg et al. 1986).

2.3. Simulated sensor bands

In situ remote sensing reflectance data were compared to the spectral bands and sensitivities of the following satellite observational systems: SPOT, Landsat-TM, MODIS, SeaWiFS, MERIS, GOCI, Alos, IRS-P6 and Rapid Eye. Spectral band response was simulated by using the arithmetic mean of the field remote sensing reflectance over the width of each spectral band to examine the CDOM estimation approaches.

2.4. Models

Many remote sensing algorithms to estimate CDOM absorption have been based on standard band-ratios, for example, R_{565}/R_{660} (Kutser et al. 2005), R_{412}/R_{670}, R_{443}/R_{670}, R_{510}/R_{670} (Del Castillo and Miller 2008), R_{412}/R_{443}, R_{490}/R_{555} (Morel and Gentili 2009).

Semi-analytical methods have also been used successfully in oceanic and coastal areas. These approaches are based on bio-optical models that link apparent optical properties (AOP) to inherent optical properties (IOPs) (Lee et al. 1994):

$$R_{rs} = \frac{ft^2}{Qn^2}\frac{b_b(\lambda)}{a(\lambda)+b_b(\lambda)} \tag{6}$$

where R_{rs} is the remote sensing reflectance of water, f is an empirical factor describing the light field, Q is the ratio of upwelling irradiance to radiance, t is the transmittance at the air-water interface, and n is the index of refraction of water. The ratio f/Q has been found to be wavelength dependent (Carder et al. 1999). One such approach, using Linear Matrix Inversion (LMI) (Hoge and Lyon 1996), has been widely applied to water color studies using hyperspectral and multiband data (IOCCG 2006; Hakvoort et al. 2002). Another approach is the QAA-CDOM model that has been successfully applied to the coastal and estuarine ecosystems (Zhu and Yu 2012).

Several multivariate models for estimation of water color variables have been used (*e.g.* Kabbara et al. 2008), which combine multispectral reflectance data and measured *in situ* optical conditions, following the form:

$$y_i = \alpha + \sum_{i=1}^{n} x_i(\lambda)\beta(\lambda) + \varepsilon_i \tag{7}$$

where y_i is the CDOM absorption of sample i, x_i is the reflectance estimated for the simulated band λ, β is the regression coefficient, α is the intercept, ε_i is the residual, and n is the total bands.

In the present study, seven empirical and two semi-analytical approaches were compared to estimate CDOM absorption at 375 nm in four, shallow, inland water bodies. Field bio-optical measurements were compared to remote sensing reflectance data and simulated satellite bands. The assessment of each model was made by comparing the estimated and measured CDOM absorption at 375 nm. The statistical analysis was performed using Origin Lab 8.0 software to determine the percentage difference (PD), bias, root mean square error (RMSE), and the coefficient of determination R^2 (Kowalczuk et al. 2010).

3. Results

3.1. Field-measured CDOM absorptions and water color variations

The sample dataset showed a range of biological and optical properties (Table 2). The Chaohu Lake had the highest CDOM absorption as well as highest TSS, OSS and Chla concentrations. The average CDOM absorption in Taihu Lake during the three measurement campaigns was not significantly different (ANOVA, $P > 0.05$). In contrast, Chla, TSS and OSS were significantly higher in the T(2008) measurement.

The minimum $a_{CDOM}(375)$ and Chla were measured in Poyang Lake. Shitoukoumen Reservoir had relatively high Chla and $a_{CDOM}(375)$ values.

3.2. Model development and validation

Standard band-ratios of the simulated multiband data were not found to correlate well with measured $a_{CDOM}(375)$ (Figure 2). Most of the CDOM absorptions at 375 nm were clustered around the range of 0–5m^{-1}. The ratios were not sensitive when the $a_{CDOM}(375)$ values were larger than 5m^{-1}. Only the R_{412}/R_{443} band-ratio provided a highest correlation ($R^2 = 0.30$).

The LMI algorithm was used to estimate $a_{CDOM}(375)$ using the T(2010) dataset and with f and Q estimated from earlier studies in the same lake: $f = 0.33$ and $Q = 3.5$ (Gons 1999). The results showed a relatively poor correlation between field and estimated CDOM values (Figure 3a). The QAA-CDOM model was used with the same dataset, to estimate $a_{CDOM}(440)$. As $a_{CDOM}(440)$ and $a_{CDOM}(375)$ is expected to be well correlated (Figure 4), we compared the estimated $a_{CDOM}(440)$ to the field $a_{CDOM}(375)$ to detect the efficiency of this method (Figure 3b). A relatively high

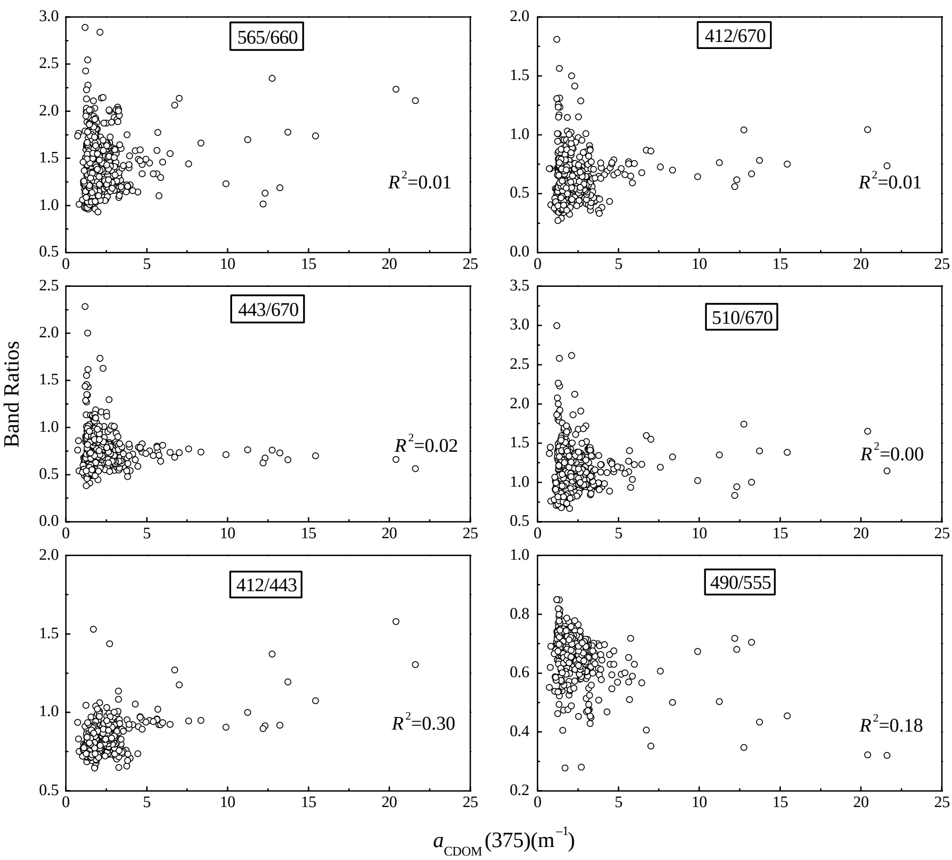

Figure 2. The distribution of different band-ratio models in relation to CDOM absorption measurements in the four study sites.

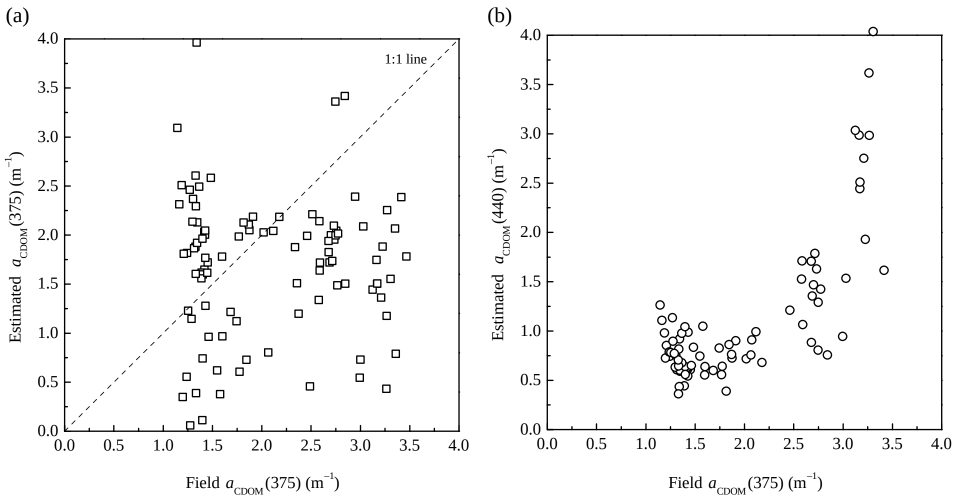

Figure 3. The semi-analytical model (LMI) (a) and QAA-CDOM method (b) applied for CDOM absorption estimation for Taihu Lake (2010 sampling campaign). Estimated $a_{CDOM}(440)$ was obtained using the QAA-CDOM model, comparing with $a_{CDOM}(375)$ used in the present study. However, the two absorptions has a significant correlation, presenting consistent results when comparing measured and estimated $a_{CDOM}(375)$.

logarithmic correlation was obtained ($R^2 = 0.62$) but the linear correlation remained low.

Multiband models were developed using hyperspectral reflectance data, at 10 nm wavelength intervals from 350–700 nm. The results showed a good correlation between estimated and measured optical data for T(2008) and T(2010) (Figure 5), with RMS errors of 20.3% and 10.8%, respectively.

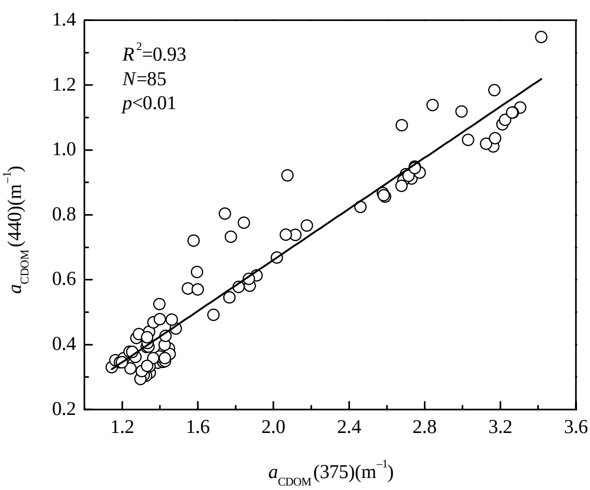

Figure 4. Results showed a significant correlation between CDOM absorptions at 375 nm and 440 nm in the dataset T(2010).

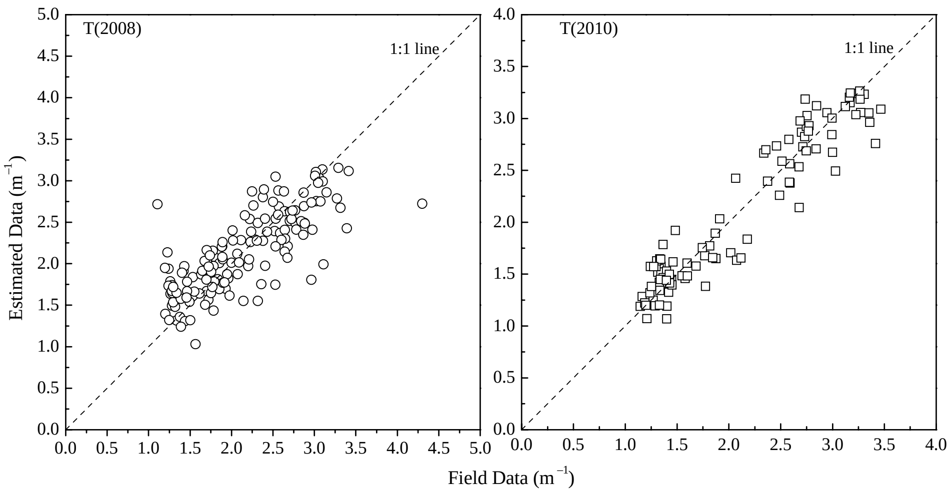

Figure 5. Comparison of estimated CDOM absorption prediction using hyperspectral data at 10 nm wavelength intervals from 350 – 700 nm, with respect to measured CDOM absorption for Taihu Lake (2008 and 2010 campaigns).

A second series of multiband models was then developed for each dataset using simulated sensor bands for the spectral characteristics of the SPOT, Landsat-TM, MODIS, SeaWiFS, MERIS, GOCI, Alos, IRS-P6 and Rapid Eye sensors systems. Data from each measurement campaign were used to evaluate the satellite sensor that could provide the best results (Table 3). The highest R^2 and lowest RMSE were consistently found using the MERIS bands, followed by GOCI and SeaWiFS. The highest R^2 and lowest RMSE were found in Chaohu Lake, the study site with highest and more variable CDOM absorptions. The poorest results occurred for the Poyang Lake data, with the lowest average CDOM.

3.3. Model utilization

The multiband model using simulated MERIS bands provided the best results for the inland waters examined (Table 3, Figure 6). To further investigate the utility of this approach, a scene of cloud-free MERIS image from 2 November 2004, was used with data from the T(2004) measurement campaign (18 October to 29 October 2004). This period was characterized by low precipitation (low inflow of allochthonous carbon) and relatively low algal production (autochthonous carbon). Therefore, the assumption was made that optical conditions were consistent over this short time period (Ortega-Retuerta et al. 2010). After geo-referencing the data, atmospheric correction was performed using the 6S model (Second Simulation of Satellite Signal in the Solar Spectrum) (Duan et al. 2008; Lee and Kaufman 1986). A comparison of *in situ* measured reflectance and satellite-derived remote sensing reflectance indicated a significant correlation between measurements ($P < 0.01$). The multiband algorithm developed for the T(2004) data was simplified, using only those bands that were significant at the 90% confidence limit. The resulting model

Table 3. The percentage difference (PD), bias, root mean square error (RMSE) and correlation coefficient between measured CDOM absorption and estimated CDOM absorption by multiband model in the study lakes.

	T(2004)				T(2008)				T(2010)				C(2009)				P(2010)				S(2008)			
Sensors	PD*	Bias	RMSE**	R^2	PD	Bias	RMSE	R^2	PD	Bias	RMSE	R^2	PD	Bias	RMSE	R^2	PD	Bias	RMSE	R^2	PD	Bias	RMSE	R^2
Landsat-TM	56	0.04	0.59	0.27	127	5.81E-04	0.48	0.44	73	5.65E-09	0.38	0.72	29	1.39E-05	2.11	0.85	43	2.74E-09	0.25	0.09	28	1.00E-08	2.22	0.39
Spot	56	0.04	0.57	0.34	120	−3.25E-03	0.54	0.28	72	−3.99E-09	0.42	0.65	31	6.07E-06	2.31	0.82	43	4.86E-09	0.25	0.07	30	1.00E-08	2.26	0.37
MODIS	57	0.04	0.57	0.33	126	1.28E-03	0.47	0.46	73	4.24E-09	0.39	0.70	27	6.06E-06	2.10	0.85	43	−1.52E-09	0.25	0.10	29	2.50E-09	2.27	0.36
SeaWiFs	60	0.03	0.53	0.41	123	8.57E-04	0.44	0.52	72	3.65E-09	0.34	0.78	26	6.06E-06	1.92	0.87	44	4.86E-09	0.23	0.22	26	1.25E-08	2.17	0.42
MERIS	58	0.02	0.45	0.58	131	−3.27E-03	0.41	0.59	79	2.48E-09	0.29	0.84	29	6.06E-06	0.90	0.97	46	−1.52E-09	0.20	0.38	29	5.25E-09	1.71	0.64
GOCI	60	0.03	0.49	0.49	130	1.71E-03	0.44	0.53	72	1.30E-09	0.34	0.78	25	6.06E-06	1.98	0.87	42	9.12E-09	0.23	0.23	30	1.25E-08	2.16	0.43
P6	55	0.04	0.58	0.33	121	−3.75E-03	0.54	0.27	72	1.54E-09	0.43	0.66	32	6.05E-06	2.28	0.82	43	2.74E-09	0.25	0.08	29	5.00E-09	2.26	0.37
Rapid Eye	57	0.02	0.54	0.40	127	2.29E-04	0.47	0.46	71	2.24E-09	0.35	0.76	27	6.06E-06	2.11	0.85	41	4.86E-09	0.24	0.12	29	5.00E-09	2.21	0.40
ALOS	57	0.04	0.59	0.29	127	1.60E-03	0.47	0.20	73	2.36E-09	0.39	0.70	28	6.05E-06	2.12	0.85	43	2.74E-09	0.25	0.10	29	7.50E-09	2.25	0.38

*The counts of PD values varying from −20 to 20%.
**The unit of RMSE is m^{-1}.

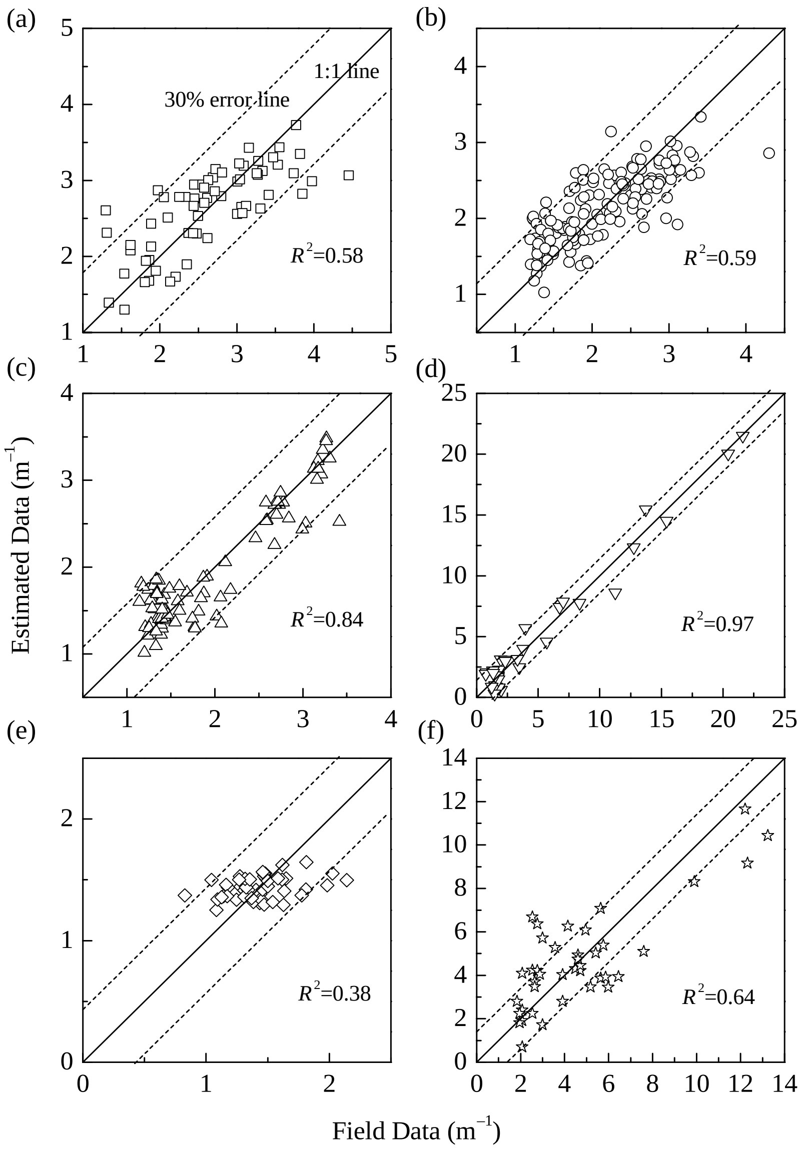

Figure 6. Comparison of field and estimated CDOM absorption coefficient at 375 nm using simulated MERIS bands in different cruises: (a) T(2004); (b) T(2008); (c) T(2010); (d) C(2009); (e) P(2010) and (f) S(2008).

was based on four bands, three in the visible and one in the infrared wavelengths of the MERIS satellite:

$$a_{\mathrm{CDOM}}(375)\left(\mathrm{m}^{-1}\right) = 1.7 - 188.25 \times \mathrm{B}_2 + 237.23 \times \mathrm{B}_3 - 126.52 \times \mathrm{B}_5 + 238.77 \times \mathrm{B}_9 \quad (8)$$

The results presented a high correlation between estimated and measured CDOM absorption. The highest correlation obtained was 0.56 with a% RMSE of 25.8%.

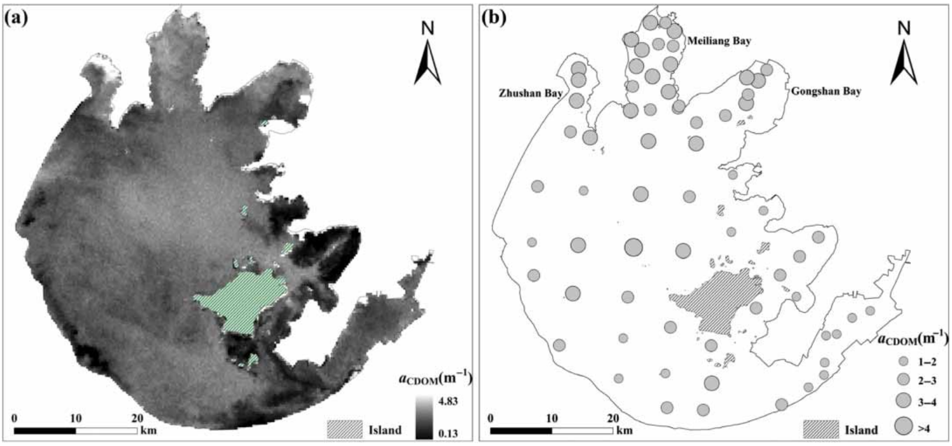

Figure 7. Geographical distribution of CDOM absorption at 375 nm in Taihu Lake in 2004 determined by (a) multiband algorithm with satellite-derived remote sensing reflectance and (b) CDOM absorption measurements.

Geographically, a close correlation was present throughout the lake with some discrepancies in the center of the lake (Figure 7). This reduction in accuracy can be attributed to disturbances by aerosols from the 6S model calibration, as this model is not perfectly suitable for atmospheric correction over large water areas, especially Case 2 waters (Vermote et al. 1997).

The spatial variation of CDOM absorption indicates that significant CDOM sources are present in northern bays: Meiliang, Zhushan and Gongshan Bays. The eastern part of the lake is characterized by lower CDOM absorption, confirming prior studies (Yao et al. 2011).

4. Discussion

Commonly used band-ratio models failed to detect CDOM absorption in the complex optical conditions of the inland water bodies examined. The semi-analytical method also did not provide satisfactory results. One reason for this may be the high spatial heterogeneity of CDOM in these lakes, caused by multiple CDOM sources and sinks. The resulting mixture of organic molecules has a wide range of molecular weights, biolability and photosensitivity (Loiselle et al. 2009). The optical conditions of these waters are further complicated by resuspension and cyanobacteria blooms (Duan et al. 2009).

The LMI method did not provide satisfactory estimates of CDOM absorption. As geometric parameters f and Q are dependent on the solar zenith angle, the viewing angle, and the azimuth difference between the solar and observational vertical direction, small variations in sampling time and geographic position, may also influence the results from this approach (Morel and Gentili 1996). Likewise, the QAA-CDOM model failed to estimate CDOM absorption. This model has been used successfully in estuarine and coastal areas, where the CDOM absorptions were lower than 1m $^{-1}$ at 440 nm and a single CDOM source usually dominates (Zhu and Yu 2012). The study lakes have an average $a_{CDOM}(440)$ of 2 m $^{-1}$, reaching more than 4 m $^{-1}$ in

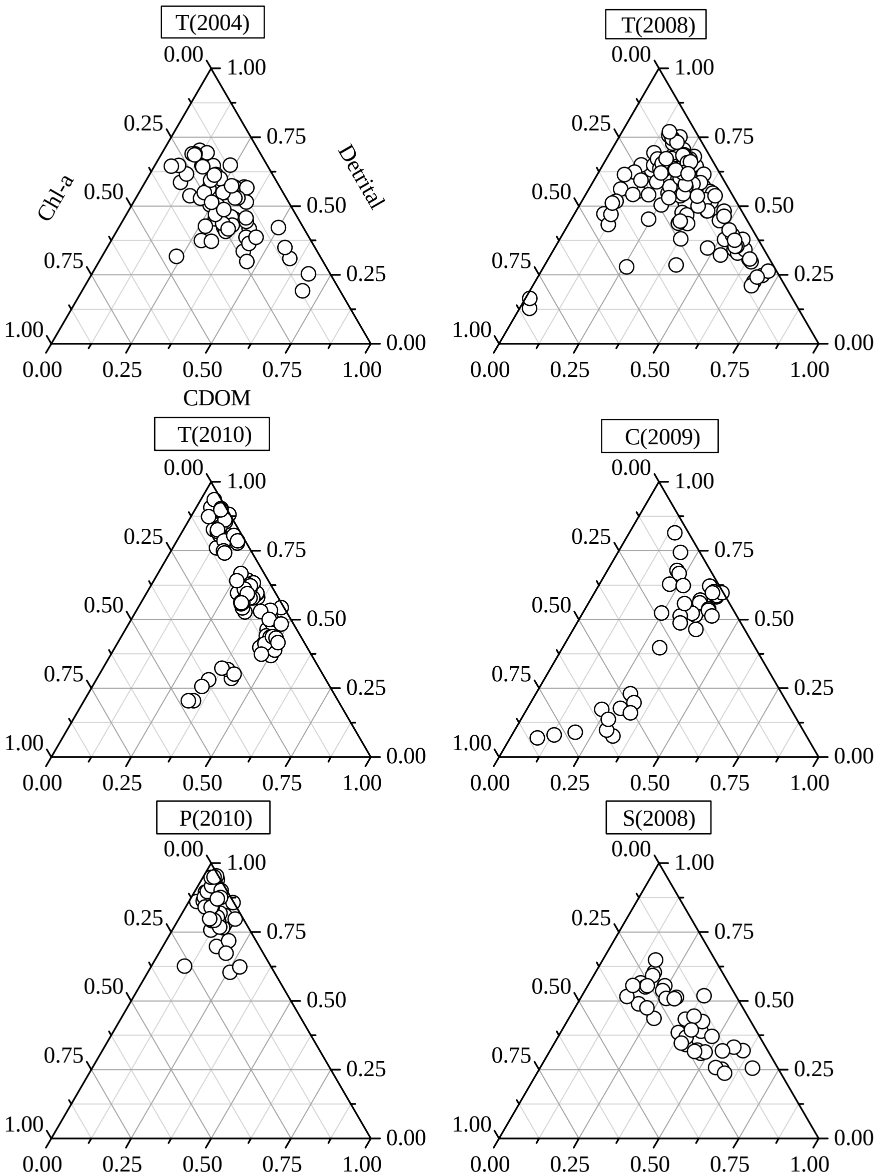

Figure 8. The contributions of optically active components to water body at 375 nm in the seven cruises with the exception of pure water (the absorptions at 375 nm of the three dominated components were normalized to the range of 0 to 1 showing the proportion of optical properties).

specific seasons. Furthermore, absorption from high concentrations of particulate matter will overlap with the absorption of CDOM, especially in the blue region, where CDOM absorption dominates the optical properties.

The success of the multiband approach in estimating CDOM absorption in the study lakes is clearly linked to the flexibility of the method and the increased

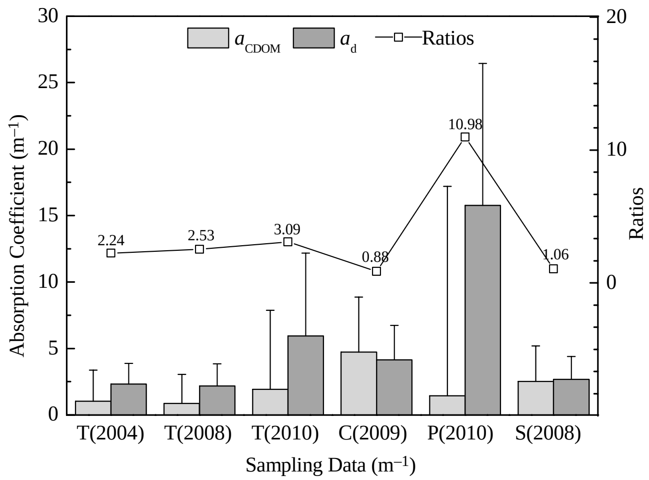

Figure 9. CDOM and detritus absorption coefficients at 375 nm and the respective average ratios between detritus and CDOM absorption coefficients.

information utilized, in particular, in infrared. Having more wavebands available allows for a reduction in the influence of particulate detritus and phytoplankton biomass (*e.g*. Lee, Carder, and Arnone 2002).

The high correlation using the simulated MERIS data was favored by the number and spectral range of the bands available. As CDOM absorption is highest in the short visible and ultraviolet wavelengths, the availability of reflectance data below 500 nm increased the possibility of associating a reduction in reflectance to CDOM absorption (Schiller and Doerffer 1999).

The multiband approach using simulated MERIS data provided statistically significant results for all lakes, with correlation coefficients showing a range of values, apparently conditioned by optically active components in the water column. The relative contribution to absorption (375 nm) by the dominant optically active components in each sampling campaign showed a wide range of optical conditions (Figure 8). In the datasets, where the multiband model gave the highest correlation, the relative weight of CDOM is above 25% and that of detrital matter below 75%. Poyang Lake has both the lowest correlation coefficient, the lowest relative CDOM absorption and the highest relative detrital absorption. The importance of particulate organic matter in overall absorption in this lake is further demonstrated by the ratio of absorption between OSS and CDOM ($\bar{a}_d/\bar{a}_g$). In Poyang Lake, this is 3 to 11 times greater than in the other study lakes (Figure 9). River discharges (Yangtze River) play a major role in the hydrological and optical conditions of the Poyang Lake (Li et al. 2010), which lower the CDOM estimation from remote sensing. In summer, extensive plumes of riverine organic matter cover much of the lake. As particulate organic matter displays similar absorption characteristics as the dissolved fraction, upwelling radiance will clearly be affected. In fact, many CDOM estimation models consider absorption from both particulate detritus and the dissolved fraction (Zhu et al. 2011).

Likewise, algal blooms will also influence CDOM estimation as several photosynthetic pigments (e.g. chlorophylls) absorb strongly in short visible wavelengths. Furthermore, algal exudates and detrital material are sources of CDOM (Yu et al. 2010). In general, the study lakes with the highest phytoplankton biomass (C(2009), T(2008), S(2008)) had a high correlation between estimate and measured CDOM absorption.

5. Conclusions

The determination of CDOM absorption and CDOM dynamics provides important information on the biogeochemical dynamics of aquatic ecosystems (Tranvik et al. 2009). However, in the complex optical conditions of Case 2 waters, the remote estimation of CDOM absorption is complicated by the presence of other optical active components. The use of semi-analytical methods requires a clear understanding of radiative transfer in conditions of high spatial and temporal heterogeneity. For this reason, empirical methods are most appropriate especially when the CDOM dominates the water color. Furthermore, the availability of a large number of bands, in particular below 500 nm appears to favor the use of these models to estimate CDOM absorption. High concentrations of algal biomass may increase the correlation between the measured and modeled CDOM absorptions due to the dominance of phytoplankton-derived CDOM sources. On the other hand, the presence of high concentrations of organic or inorganic detritus will reduce our ability to estimate CDOM absorption in Case 2 waters. Understanding CDOM dynamics in these ubiquitous shallow waters is fundamental to understanding the role they play in global carbon balances. Clearly the availability of hyperspectral satellite data is fundamental to improving our knowledge of these ecosystems.

Acknowledgments

We gratefully acknowledge the financial support of the Knowledge Innovation Program of the Chinese Academy of Sciences (Grant No.KZCX2-YW-QN311, No.KZCX2-EW-QN308), National Natural Science Foundation of China (Grant No.40871168, No.40801137), and the Dragon 3 Projects (ID-10561). We thank Guofeng Wu, Wen Su, Linlin Shang, Lin Zhou, Chunguang Lv, Jiawang Rao and Chenlu Zhao for participating in the field campaigns and experiment analysis. We would like to thank the two anonymous reviewers for their suggestions which greatly improved this manuscript.

References

Bélanger, S., M. Babin, and P. Larouche. 2008. "An Empirical Ocean Color Algorithm for Estimating the Contribution of Chromophoric Dissolved Organic Matter to Total Light Absorption In Optically Complex Waters." *Journal of Geophysical Research* 113 (C4): C04027. doi:10.1029/2007JC004436.

Briucaud A., A. Morel, and L. Prieur. 1981. "Absorption by Dissolved Organic Matter of the Sea (Yellow Substance) in the UV and Visible Domains." *Limnology and Oceanography* 26 (1): 43–53. doi:10.4319/lo.1981.26.1.0043.

Carder, K. L., F. R. Chen, Z. P. Lee, S. K. Hawes, and D. Kamykowski. 1999. "Semianalytic Moderate-Resolution Imaging Spectrometer Algorithms for Chlorophyll *a* and Absorption with Bio-Optical Domains Based on Nitrate-Depletion Temperatures." *Journal of Geophysical Research* 104 (C3): 5403–5421. doi:10.1029/1998JC900082.

Del Castillo, C. E., and R. L. Miller. 2008. "On the Use of Ocean Color Remote Sensing to Measure the Transport of Dissolved Organic Carbon by the Mississippi River Plume." *Remote Sensing of Environment* 112 (3): 836–844. doi:10.1016/j.rse.2007.06.015.

Duan, H., Y. Zhang, B. Zhang, K. Song, Z. Wang, D. Liu, and F. Li. 2008. "Estimation of Chlorophyll-*a* Concentration and Trophic States for Inland Lakes in Northeast China from Landsat TM Data and Feld Spectral Measurements." *International Journal of Remote Sensing* 29 (3): 767–786. doi:10.1080/01431160701355249.

Duan, H., R. Ma, X. Xu, F. Kong, S. Zhang, W. Kong, J. Hao, and L. Shang. 2009. "Two-Decade Reconstruction of Algal Blooms in China's Lake Taihu." *Environmental Science & Technology* 43 (10): 3522–3528. doi:10.1021/es8031852.

Duan, H. T., R. H. Ma, Y. Z. Zhang, S. A. Loiselle, J. P. Xu, C. L. Zhao, L. Zhou, and L. L. Shang. 2010. "A New Three-Band Algorithm for Estimating Chlorophyll Concentrations in Turbid Inland Lakes." *Environmental Research Letters* 5 (4): 044009. doi:10.1088/1748-9326/5/4/044009.

Gersberg, R. M., B. V. Elkins, S. R. Lyon, and C. R. Goldman. 1986. "Role of Aquatic Plants in Wastewater Treatment by Artificial Wetlands." *Water Research* 20 (3): 363–368. doi:10.1016/0043-1354(86)90085-0.

Gons, H. J. 1999. "Optical Teledetection of Chlorophyll *a* in Turbid Inland Waters." *Environment Science & Technology* 33 (7): 1127–1132. doi:10.1021/es9809657.

Hakvoort, H., J. de Haan, R. Jordans, R. Vos, S. Peters, and M. Rijkeboer. 2002. "Towards Airborne Remote Sensing of Water Quality in the Netherlands-Validation and Error Analysis." *ISPRS Journal of Photogrammetry & Remote Sensing* 57 (3): 171–183. doi:10.1016/S0924-2716(02)00120-X.

Hoge, F. E., and P. E. Lyon. 1996. "Satellite Retrieval of Inherent Optical Properties by Liner Matrix Inversion of Oceanic Radiance Models: An Analysis of Model and Radiance Measurement Errors." *Journal of Geophysical Research* 101 (C7): 16631–16648. doi:10.1029/96JC01414.

IOCCG. 2006. "Remote Sensing of Inherent Optical Properties: Fundamentals, Tests of Algorithms, and Applications." In *Reports of the International Ocean-Colour Coordinating Group, No. 5*, edited by Z. P. Lee, 49–56. Dartmouth: IOCCG.

Jiang, G., D. Liu, K. Song, Z. Wang, B. Zhang, and Y. Wang. 2010. "Application of Multivariate Model Based on Three Simulated Sensors for Water Quality Variables Estimation in Shitoukoumen Reservoir, Jilin Province, China." *Chinese Geographical Science* 20 (4): 337–344. doi:10.1007/s11769-010-0406-4.

Kabbara, N., J. Benkhelil, M. Awad, and V. Barale. 2008. "Monitoring Water Quality in the Coastal Area of Tripoli (Lebanon) Using High-Resolution Satellite Data." *ISPRS Journal of Photogrammetry and Remote Sensing* 63 (5): 488–495. doi:10.1016/j.isprsjprs.2008.01.004.

Kirk, J. T. O. 1976. "Yellow Substance (Gelbstoff) and its Contribution to the Attenuation of Photosynthetically Active Radiation in Some Inland and Coastal South-Eastern Australian Waters." *Australian Journal of Marine & Freshwater Research* 27 (1): 61–71. doi:10.1071/MF9760061.

Kowalczuk, P., W. J. Cooper, R. F. Whitehead, M. J. Durako, and W. Sheldon. 2003. "Characterization of CDOM in an Organic-Rich River and Surrounding Coastal Ocean in the South Atlantic Bight." *Aquatic Sciences* 65 (4): 384–401. doi:10.1007/s00027-003-0678-1.

Kowalczuk, P., M. Darecki, M. Zablocka, and I. Górecka. 2010. "Validation of Empirical and Semi-Analytical Remote Sensing Algorithms for Estimating Absorption by Coloured Dissolved Organic Matter in the Baltic Sea from SeaWiFS and MODIS Imagery." *Oceanologia* 52 (2): 171–196. doi:10.5697/oc.52-2.171.

Kutser, T., D. C. Pierson, L. Tranvik, A. Reinart, S. Sobek, and K. Kallio. 2005. "Using Satellite Remote Sensing to Estimate the Colored Dissolved Organic Matter Absorption Coefficient in Lakes." *Ecosystems* 8 (6): 709–720. doi:10.1007/s10021-003-0148-6.

Lee, T., and Y. Kaufman. 1986. "Non-Lambertian Effects on Remote-Sensing of Surface Reflectance and Vegetation Index." *IEEE Transactions on Geoscience and Remote Sensing* 24 (5): 699–708. doi:10.1109/TGRS.1986.289617.

Lee, Z., and K. L. Carder. 2004. "Absorption Spectrum of Phytoplankton Pigments Derived from Hyperspectral Remote-Sensing Reflectance." *Remote Sensing of Environment* 89 (3): 361–368. doi:10.1016/j.rse.2003.10.013.

Lee, Z., K. L. Carder, S. K. Hawes, R. G. Steward, T. G. Peacock, and C. O. Davis. 1994. "Model for the Interpretation of Hyperspectral Remote-Sensing Reflectance." *Applied Optics* 33 (24): 5721–5732. doi:10.1364/AO.33.005721.

Lee, Z., K. L. Carder, and R. A. Arnone. 2002. "Deriving Inherent Optical Properties from Water Color: A Multiband Quasi-Analytical Algorithm for Optically Deep Waters." *Applied Optics* 41 (27): 5755–5772. doi:10.1364/AO.41.005755.
Li, H., X. L. Chen, K. J. Lim, X. B. Cai, and M. Sagong. 2010. "Assessment of Soil Erosion and Sediment Yield in Liao Watershed, Jiangxi Province, China, Using USLE, GIS, and RS." *Journal of Earth Science* 21 (6): 941–953. doi:10.1007/s12583-010-0147-4.
Loiselle, S. A., N. Azza, J. Gichuki, L. Bracchini, A. Tognazzi, A. M. Dattilo, C. Rossi, and A. Cozar. 2010. "Spatial Dynamics of Chromophoric Dissolved Organic Matter in Nearshore Waters of Lake Victoria." *Aquatic Ecosystem Health & Management* 13 (2): 185–195. doi:10.1080/14634988.2010.481236.
Loiselle, S. A., L. Bracchini, A. Cózar, A. M. Dattilo, A. Tognazzi, and C. Rossi. 2009. "Variability in Photobleaching Rates and Their Related Impacts on Optical Conditions in Subtropical Lakes." *Journal of Photochemistry and Photobiology B: Biology* 95 (2): 129–137. doi:10.1016/j.jphotobiol.2009.02.002.
Loiselle, S., D. Vione, C. Minero, V. Maurino, A. Tognazzi, A. M. Dattilo, C. Rossi, and L. Bracchini. 2012. "Chemical and Optical Phototransformation of Dissolved Organic Matter." *Water Research* 46 (10): 3197–3207. doi:10.1016/j.watres.2012.02.047.
Ma, R. H., H. T. Duan, C. M. Hu, X. Z. Feng, A. N. Li, W. M. Ju, J. H. Jiang, and G. S. Yang. 2010. "A Half-Century of Changes in China's Lakes: Global Warming or Human Influence?" *Geophysical Research Letters* 37: L24106. doi:10.1029/2010GL045514.
Ma, R., G. Jiang, H. Duan, L. Bracchini, and S. Loiselle. 2011. "Effective Upwelling Irradiance Depths in Turbid Waters: A Spectral Analysis of Origins and Fate." *Optics Express* 19 (8): 7127–7138. doi:10.1364/OE.19.007127.
Miller, R. L., M. Belz, C. D. Castillo, and R. Trzaska 2002. "Determining CDOM Absorption Spectra in Diverse Coastal Environments Using a Multiple Pathlength, Liquid Core Waveguide System." *Continental Shelf Research* 22 (9): 1301–1310. doi:10.1016/S0278-4343(02)00009-2.
Mobley, C. D. 1999. "Estimation of the Remote-Sensing Reflectance from Above-Surface Measurements." *Applied Optics* 38 (36): 7442–7455. doi:10.1364/AO.38.007442.
Morel, A., and B. Gentili. 1996. "Diffuse Reflectance of Oceanic Waters. III. Implication of Bidirectionality for the Remote-Sensing Problem." *Applied Optics* 35 (24): 4850–8462. doi:10.1364/AO.35.004850.
Morel, A., and B. Gentili. 2009. "A Simple Band Ratio Technique to Quantify the Colored Dissolved and Detrital Organic Material from Ocean Color Remotely Sensed Data." *Remote Sensing of Environment* 113 (5): 998–1011. doi:10.1016/j.rse.2009.01.008.
Morel, A., and L. Prieur. 1977. "Analysis of Variations in Ocean Color." *Limnology and Oceanography* 22 (4): 709–722. doi:10.4319/lo.1977.22.4.0709.
Morel, A. 1988. "Optical Modeling of the Upper Ocean in Relation to Its Biogenous Matter Content (Case I Waters)." *Journal of Geophysical Research* 93 (C9): 10749–10768. doi:10.1029/JC093iC09p10749.
Mueller, J. L., G. S. Fargion, and C. R. Mcclain. 2003. *Ocean Optics Protocols for Satellite Ocean Color Sensor Validation*, Revision 4. Greenbelt, MD: National Aeronautics and Space Administration, Goddard Space Flight Center.
Ortega-Retuerta, E., D. A. Siegel, N. B. Nelson, C. M. Duarte, and I. Reche. 2010. "Observations of Chromophoric Dissolved and Detrital Organic Matter Distribution Using Remote Sensing in the Southern Ocean: Validation, Dynamics and Regulation." *Journal of Marine Systems* 82 (4): 295–303. doi:10.1016/j.jmarsys.2010.06.004.
Schiller, H., and R. Doerffer. 1999. "Neural Network for Emulation of an Inverse Model-Operational Derivation of Case II Water Properties from MERIS Data." *International Journal of Remote Sensing* 20 (9): 1735–1746. doi:10.1080/014311699212443.
Siegel, D. A., S. Maritorena, N. B. Nelson, D. A. Hansell, and M. Lorenzi-Kayser. 2002. "Global Distribution and Dynamics of Colored Dissolved and Detrital Organic Materials." *Journal of Geophysical Research* 117 (C12): 3228. doi:10.1029/2001JC000965.
Stedmon, C. A., S. Markager, and R. Bro. 2003. "Tracing Dissolved Organic Matter in Aquatic Environments Using a New Approach to Fluorescence Spectroscopy." *Marine Chemistry* 82 (3–4): 239–254. doi:10.1016/S0304-4203(03)00072-0.

Tranvik, L. J., J. A. Downing, J. B. Cotner, S. A. Loiselle, R. G. Striegl, T. J. Ballatore, P. Dillon, et al. 2009. "Lakes and Reservoirs as Regulators of Carbon Cycling and Climate." *Limnology and Oceanography* 54: 2298–2314. doi:10.4319/lo.2009.54.6_part_2.2298.

Vermote, E. F., D. Tanre, J. L. Deuze, M. Herman, and J. J. Morcette. 1997. "Second Simulation of the Satellite Signal in the Solar Spectrum, 6S: An Overview." *IEEE Geoscience and Remote Sensing Society* 35 (3): 675–686. doi:10.1109/36.581987.

Xie, L., P. Xie, L. Guo, L. Li, Y. Miyabara, and H.-D. Park. 2005. "Organ Distribution and Bioaccumulation of Microcystins in Freshwater Fish at Different Trophic Levels from the Eutrophic Lake Chaohu." *China, Environmental Toxicology* 20 (3): 293–300. doi:10.1002/tox.20120.

Yao, X., Y. Zhang, G. Zhu, B. Qin, L. Feng, L. Cai, and G. Gao. 2011. "Resolving the Variability of CDOM Fluorescence to Differentiate the Sources and Fate of DOM in Lake Taihu and Its Tributaries." *Chemosphere* 82 (2): 145–155. doi:10.1016/j.chemosphere.2010.10.049.

Yu, Q., Y. Q. Tian, R. F. Chen, A. Liu, G. B. Gardner, and W. Zhu. 2010. "Functional Linear Analysis of *In Situ* Hyperspectral Data for Assessing CDOM in Rivers." *Photogrammetric Engineering & Remote Sensing* 76 (10): 1147–1158.

Zhu, W., and Q. Yu. 2012. "Inversion of Chromophoric Dissolved Organic Matter (CDOM) from EO-1 Hyperion Imagery for Turbid Estuarine and Coastal Waters." *IEEE Transactions on Geosciences and Remote Sensing* 99: 1–13. doi:10.1109/TGRS.2012.2224117.

Zhu, W., Q. Yu, Y. Q. Tian, R. F. Chen, and G. B. Gardner. 2011. "Estimation of Chromophoric Dissolved Organic Matter in the Mississippi and Atchafalaya River Plume Regions Using Above-Surface Hyperspectral Remote Sensing." *Journal of Geophysical Research* 116 (C2): C02011. doi:10.1029/2010JC006523.